



Chemistry A European Journal

 **Chemistry
Europe**
European Chemical
Societies Publishing

Accepted Article

Title: Construction of helical structures with multiple fused anthracenes: structures and properties of long expanded helicenes

Authors: Kei Fujise, Eiji Tsurumaki, Kan Wakamatsu, and Shinji Toyota

This manuscript has been accepted after peer review and appears as an Accepted Article online prior to editing, proofing, and formal publication of the final Version of Record (VoR). This work is currently citable by using the Digital Object Identifier (DOI) given below. The VoR will be published online in Early View as soon as possible and may be different to this Accepted Article as a result of editing. Readers should obtain the VoR from the journal website shown below when it is published to ensure accuracy of information. The authors are responsible for the content of this Accepted Article.

To be cited as: *Chem. Eur. J.* 10.1002/chem.202004720

Link to VoR: <https://doi.org/10.1002/chem.202004720>

WILEY-VCH

COMMUNICATION

Construction of helical structures with multiple fused anthracenes: structures and properties of long expanded helicenes

Kei Fujise,^[a] Eiji Tsurumaki,^[a] Kan Wakamatsu,^[b] Shinji Toyota*^[a]

[a] K. Fujise, Dr. E. Tsurumaki, Prof. Dr. S. Toyota
Department of Chemistry, School of Science
Tokyo Institute of Technology
2-12-1 Ookayama, Meguro-ku, Tokyo 152-8551 (Japan)
E-mail: stoyota@chem.titech.ac.jp

[b] Prof. Dr. K. Wakamatsu
Department of Chemistry, Faculty of Science
Okayama University of Science
1-1 Ridaicho, Kita-ku, Okayama 700-0005, (Japan)

Supporting information and the ORCID identification numbers for the authors of this article can be found via a link at the end of the document.

Abstract: Polycyclic aromatic compounds consisting of four or five fused anthracene units were synthesized by PtCl₂-catalyzed cycloisomerization as novel long expanded helicenes. These compounds have helical structures with significant stacking of the terminal anthracene moieties at 0.33 nm interlayer distance. In the UV-vis and fluorescence spectra, the absorption and emission bands were red-shifted as the number of fused anthracene units was increased. The characteristic broad and long-lived emission bands of the long analogs are explained by the excimer-like stabilization of the excited state. These photophysical data as well as their cyclic voltammetric data are discussed on the basis of the π -conjugation and interlayer π ··· π interactions in the molecular structures and the molecular orbitals. The barrier and mechanism of helical inversion are also reported.

In the chemistry of helicenes, researchers have continued their efforts to synthesize long analogs by adding benzene units to realize novel structures and properties.^[1,2] The helical structure of the longest helicene, [16]helicene, has more than 2.5 turns, and some benzene units are triply layered.^[3] Recently, we reported new aromatic compound [3]HA (hereinafter, [n]HA refers to a helical anthracene with n fused anthracene units) as an expanded helicene,^[4] which is defined as a helicene with extra linearly fused benzene rings into angularly fused units (Figure 1).^[5,6] Even though the racemization via helical inversion takes place rapidly for [3]HA, the barrier is sufficiently enhanced by the introduction of diphenyl substituents enough to enable resolution of its enantiomers at room temperature. We found that these enantiomers exhibited considerably intense circular dichroism and circularly polarized luminescence activities for simple organic molecules.^[7,8] In [3]HA, the number of turns is approximately one and the terminal benzene rings interact with each other but do not completely overlap. The introduction of additional anthracene units into [3]HA should increase the number of helical turns exceed one, leading to significant interactions between the anthracene units in a face-to-face fashion. Such interactions across the helical turns should influence the structures and

properties of the π -conjugated system. We were interested in how the structures and the photophysical properties are influenced by the introduction of additional anthracene units into the helical system, and designed [4]HA and [5]HA having four and five anthracene units, respectively. The synthesis of these compounds is challenging because their structures can be regarded as a substructure of helically twisted nanographenes^[9] or molecular springs.^[6,10] We herein report the synthesis of these long helical anthracenes and compare their structures, properties, and dynamic behavior involving helical inversion with those of anthracene (A), [2]HA (antra[2,1-a]anthracene), and [3]HA.

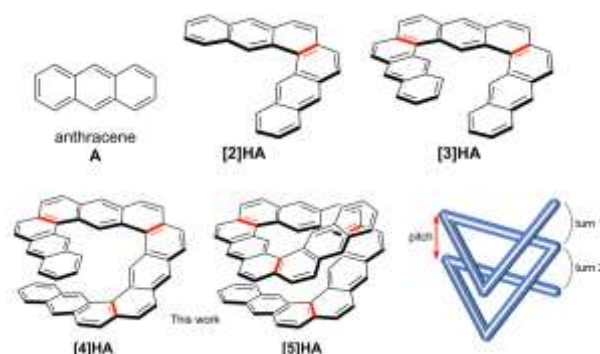
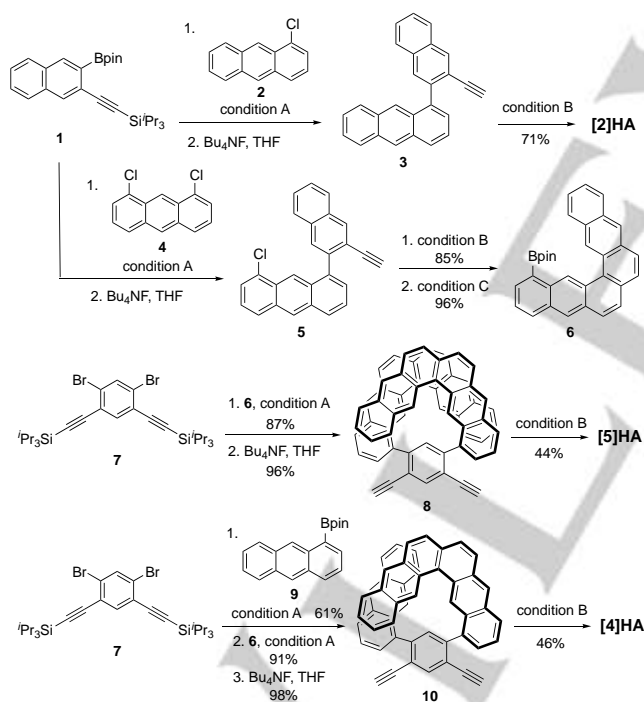


Figure 1. Structures of anthracene (A) and helical anthracenes ([n]HA), and a schematic presentation of a helical structure. Fused sides are highlighted in red.

The target compounds were synthesized by cycloaromatization of terminal alkyne precursors prepared by the Suzuki-Miyaura coupling of suitable arene building units, as was adopted for the synthesis of [3]HA.^[4] The synthetic routes are shown in Scheme 1. Compound [2]HA, which had been synthesized by photocyclization previously,^[11] was synthesized by the cycloaromatization approach. The precursor of [2]HA was prepared by the Suzuki-Miyaura coupling of 1 and 1-

COMMUNICATION

chloroanthracene (**2**)^[12] followed by desilylation. Compound **3** was heated at 80 °C for 24 h in the presence of PtCl₂ and P(C₆F₅)₃ to give **[2]HA** in 71% isolated yield.^[13] Compound **6**, a substituted analog of **[2]HA**, was prepared from **1** and 1,8-dichloroanthracene (**4**) in a similar manner followed by Pd-catalyzed borylation. The Suzuki-Miyaura coupling of **6** and dibromobenzene **7** in 2:1 ratio followed by desilylation afforded terminal alkyne **8**. Cyclization of this precursor afforded **[5]HA** in 44% isolated yield as an orange solid. For the precursor of **[4]HA**, two kinds of aryl units **9** and **6** were introduced into **7** by coupling reactions. Cyclization of **10** afforded **[4]HA** in 46% isolated yield as a yellow solid. Although **[4]HA** and **[5]HA** were less stable than **[3]HA** and slowly decomposed in solution under ambient conditions, we were able to isolate these long analogs and measure their spectroscopic data by taking the necessary precautions. Compounds **[4]HA** and **[5]HA** were characterized by ¹H NMR and mass spectral measurements. These compounds showed signals in the aromatic region of the ¹H NMR spectra as expected for the symmetric structures.^[14] The signals due to the inner hydrogen atoms in the nonterminal anthracene units were observed at 12.6 ppm for **[4]HA** and 12.5 and 13.3 (central) ppm for **[5]HA** (cf. 12.11 ppm for **[3]HA**).^[4] These hydrogen atoms were extraordinarily deshielded as ordinary neutral aromatic compounds because of the enhanced ring current effect of the aromatic moieties.



Scheme 1. Synthesis of target compounds **[2]HA**, **[4]HA**, and **[5]HA**. Condition A: Pd₂(dba)₃·CHCl₃, SPhos, and K₂CO₃ in toluene/H₂O/1,4-dioxane. Condition B: PtCl₂ and P(C₆F₅)₃ in toluene. Condition C: (Bpin)₂, Pd₂(dba)₃, SPhos, and KOAc in 1,4-dioxane. For detailed conditions, see Supporting Information.

A single crystals of **[4]HA** suitable for X-ray analysis was obtained as racemic crystals and the structures of *P*-helicity are shown in Figure 2. The molecule takes a helical structure of approximately C₂ symmetry. The terminal anthracene units are stacked on top of each other but do not completely overlap. The

interlayer distance between the terminal anthracene units, which was calculated from the coordinates of the carbon atoms around benzene rings B and K, is 0.36–0.37 nm and regarded as the pitch of the central helix. This value is comparable to the calculated pitches of *[n]*helicenes (ca. 0.37 nm for *n* = 11–14).^[3,9a,10a,15] The shortest nonbonding C···C distance between the layered anthracene units, 0.332 nm for C6···C22, is comparable to the sum of the van der Waals radii of C(sp²) atoms. This molecule has three *[4]*helicene substructures around benzenes B–E, E–H, and H–K, in which the torsion angles along the inner carbon rims are in the range of +8.6 to +21.4°. Therefore, the stereochemistry of this structure is *P* for the overall molecule (global helicity), and *P,P,P* for the three *[4]*helicene moieties (local helicity). We calculated the HOMA (Harmonic Oscillator Model of Aromaticity) index for each benzene ring from the X-ray structures. The values are 0.72–0.80 for the terminal and linearly fused benzene rings (A, B, E, H, K, and L) and 0.29–0.47 for the angularly fused benzene rings (C, D, F, G, I, and J), indicating that the π-conjugation is less effective in the latter.

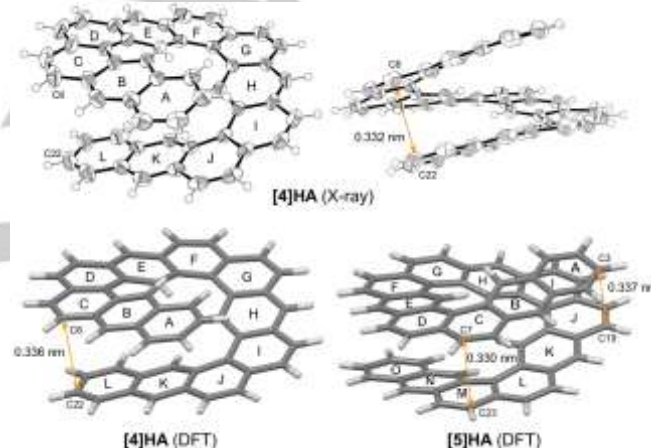


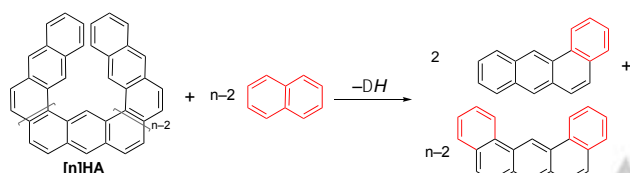
Figure 2. X-ray structures of **[4]HA** (ORTEP: 50% probability) and calculated structures of **[4]HA** and **[5]HA** at M06-2X/6-31G(d,p) level. The structures of *P* global helicity are shown.

The X-ray structure of **[4]HA** was reproduced by DFT calculations at the M06-2X/6-31G(d,p) level (Figure 2).^[16,17] The global minimum structure of C₂ symmetry has the local helicity of *P,P,P*, which is slightly more stable than the other energy-minimum structure of the *P,P,M* form. The calculations of **[5]HA** gave two energy-minimum structures having comparable energies; one is C₂ symmetric (Figure 2) and the other is less symmetric.^[18] The two terminal anthracene units on both sides are nearly double layered with each other. The typical short interlayer C···C distances (ca. 0.33 nm) are shown in the optimized structures. The number of helical turns of **[5]HA** is ca. 1.5, which is unambiguously smaller than the ideal value (1.67) expected for the planar triangular structure due to torsional deformation. The torsion angles around the four *[4]*helicene substructures are in the range of +10.7° to +17.2°, meaning that the local helicity is *P,P,P,P*. In the other stable structure, one of the nonterminal *[4]*helicene units is nearly coplanar.

The stability of the helical molecules was analyzed by using the homodesmotic reaction shown in Scheme 2, where the products consisted of planar and non-strained

COMMUNICATION

benzoanthracenes.^[10a,19] The enthalpies of reaction ($-\Delta H$) calculated at the M06-2X/6-31G(d,p) level were 35.5 ([2]HA), 63.3 ([3]HA), 69.7 ([4]HA), 67.5 ([5]HA), and 65.5 ([6]HA) kJ mol^{-1} . The positive values mean that the reactants involving an [n]HA molecule are less stable than the products. The increase of the enthalpy of reaction from [2]HA to [3]HA is mainly attributed to the increased steric strain resulting from the out-of-plane deformation. In contrast, the values are nearly the same for [n]HA ($n = 3-6$) even though a deformed anthracene unit is added successively. This indicates that the destabilization by the steric strain is almost cancelled by the stabilization by the $\pi \cdots \pi$ interactions in [4]HA and the long analogs. This factor is supported by the calculated binding energy of a face-to-face stacked anthracene dimer (35–42 kJ mol^{-1}).^[20] Therefore, attractive interactions should play an important role in the layered anthracene moieties in the long analogs. These structural and thermochemical features are well visualized by noncovalent interaction (NCI) analysis (Figure 3).^[21] The green isosurface showing weak interactions spreads over the stacked anthracene moieties in [4]HA and [5]HA, in contrast to the very limited isosurface in [3]HA.



Scheme 2. Homodesmotic reaction for estimation of strain and attractive energies of [n]HA.

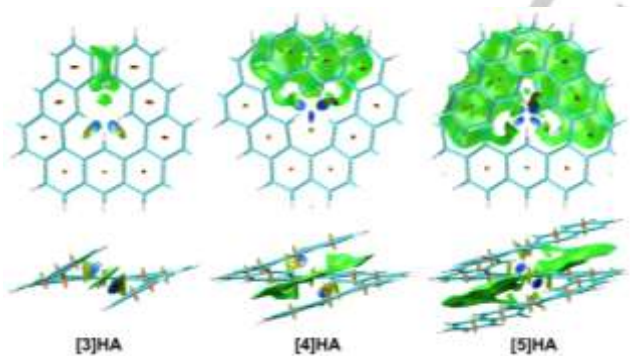


Figure 3. NCI plots (isosurface value 0.5) of stable C_2 symmetric structures of [3]HA, [4]HA, and [5]HA. Green isosurface shows regions having noncovalent (van der Waals) interactions. Blue and red isosurfaces show regions having attractive and repulsive interactions, respectively (See also Figure S13).

The UV-vis and fluorescence spectra of [4]HA and [5]HA were measured in CHCl_3 at room temperature. These data were compared with those of the other compounds, as shown in Figure 4 and Table 1. Compounds [4]HA and [5]HA generated broad and continuous shoulder bands from 330 nm to 500 nm in the UV-vis spectra. Because the absorption maxima at the longest wavelength were not clear, we compared the onset wavelengths. The wavelengths were red-shifted from 391 nm (A) to 514 nm ([5]HA) as the number of anthracene units increased. This tendency is consistent with the calculated HOMO-LUMO gaps

that decreased as the number of anthracene units increased (Table 1). In the fluorescence spectra, [4]HA and [5]HA showed weak emission bands ($\Phi_f < 0.10$) at long wavelengths (500–650 nm). These emission bands are significantly broad and long-lived compared with the emission bands of the other compounds.^[22] In addition, [4]HA and [5]HA have large Stokes shifts of 2,400 cm^{-1} . These features mean that the excited state of the long analogs should be stabilized by the interlayer interactions in an excimer-like manner.^[23,24] In fact, the interlayer separations in [4]HA and [5]HA are narrowed by ca. 0.004–0.009 nm in the optimized structures at S_1 excited state compared with those at S_0 ground state (Figure S10).

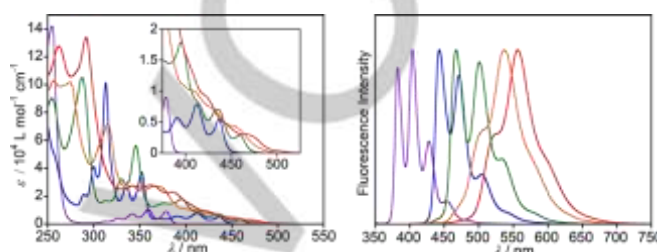


Figure 4. UV-vis (left) and fluorescence (right) spectra of anthracene A (purple), [2]HA (blue), [3]HA (green), [4]HA (orange), and [5]HA (red) in CHCl_3 at room temperature.

In order to investigate the electrochemical properties, we conducted cyclic voltammetry measurements of the series of compounds. Compounds [4]HA and [5]HA exhibited two reversible oxidation waves, whereas [2]HA and [3]HA exhibited only one wave (Figure S7). The first oxidation potential E_{ox}^1 continuously decreased as the number of anthracene units increased. These data mean that the long analogs are readily oxidized to form relatively stable oxidized species. This trend is consistent with the calculated HOMO levels that increased as the number of anthracene units increased (Table 1 and Figure S9).

Regardless of the chiral structures of [4]HA and [5]HA, we failed to resolve their enantiomers by chiral HPLC at room temperature. Thus, the helical inversion process was analyzed by DFT calculations. The global minimum structure of [4]HA was converted into its enantiomeric structure by the stepwise mechanism shown in Figure 5. The first inversion takes place at a terminal [4]helicene moiety with a relatively low barrier, and the second inversion takes place at the central [4]helicene moiety via the C_s symmetric transition state. The following inversion at the remaining terminal [4]helicene moiety completes the enantiomerization. The barrier to helical inversion was calculated to be ΔG^\ddagger 95.3 kJ mol^{-1} for [4]HA. This barrier is not sufficiently high to resolve the enantiomers at room temperature. The helical inversion of [5]HA takes place in a stepwise fashion via four intermediates. The barrier to the overall process was estimated to be ca. 110 kJ mol^{-1} , even though the least stable transition state structure could not be fully optimized. Because of this high barrier, the unsuccessful resolution was attributable to poor separation as well as low stability. The barriers to helical inversion increased in the order of [2]HA (21.8 kJ mol^{-1}) < [3]HA (25.2 kJ mol^{-1})^[4] << [4]HA < [5]HA. The introduction of the fourth unit considerably enhanced the barrier because of the destabilization of the transition state by steric interactions between the terminal moieties. These barriers of [4]HA and [5]HA are lower than those

COMMUNICATION

Table 1. Photophysical, electrochemical, and DFT calculation data of anthracene (**A**) and **[n]HA** analogs.

| | UV-vis ^[a] | | FL ^[a] | | | Stokes shift [cm ⁻¹] | DFT ^[e] | | CV <i>E</i> _{ox} [V] | |
|--------------|-----------------------|---|----------------------------|-----------------------|----------------------------|-------------------------------------|--------------------|-----------|----------------------------------|----------------------|
| | λ_{\max} [nm] | λ_{onset} [nm (eV)] ^[b] | λ_{em} [nm] | Φ ^[c] | τ [ns] ^[d] | | HOMO [eV] | LUMO [eV] | | HOMO–LUMO [eV] |
| A | 379 | 391 (3.17) | 383, 404 | 0.12 | 2.0 | 276 | –5.26 | –1.61 | 3.66 | +1.00 ^[f] |
| [2]HA | 437 | 455 (2.72) | 443, 471 | 0.46 | 16.4 | 310 | –5.03 | –1.90 | 3.13 | +0.67 |
| [3]HA | 459 | 478 (2.59) | 467, 501 | 0.18 | 9.6 | 373 | –4.92 | –1.94 | 2.97 | +0.61 |
| [4]HA | 450 | 497 (2.50) | 505, 537 | 0.084 | 14.2 | 2420 | –4.81 | –2.05 | 2.76 | +0.48, +0.79 |
| [5]HA | 467 | 514 (2.41) | 526, 556 | 0.052 | 16.9 | 2400 | –4.72 | –2.06 | 2.67 | +0.39, +0.68 |
| [6]HA | | | | | | | –4.65 | –2.03 | 2.62 | |

[a] Measured in CHCl₃ at 1.0×10^{-5} mol L⁻¹ (UV-vis) and $1.0\text{--}2.9 \times 10^{-5}$ mol L⁻¹ (FL). [b] Determined from band onset at $\epsilon = 100$ L mol⁻¹ cm⁻¹. [c] Absolute fluorescence quantum yield. [d] Fluorescence lifetime. [e] At B3LYP/6-31G(d,p)//M06-2X/6-31G(d,p) level. [f] An Irreversible wave.

of **[n]helicenes** ($n = 8\text{--}10$, 180–210 kJ mol⁻¹) as helical structures with ca. 1.5 turns.^[25] Therefore, the fused anthracene system having a large helical diameter is flexible during the helical inversion process compared with the parent helicene system.

resolve their enantiomers, we need to modify the structures to enhance the racemization barrier as well as the stability and solubility. Further extension of the anthracene units remains a challenge in the generation of enantiopure helical anthracenes and in testing their performance as molecular springs, for example their contraction-expansion behavior, by spectroscopic measurements at high pressure. The synthesis and structural modification of such molecules having a large number of turns are in progress.

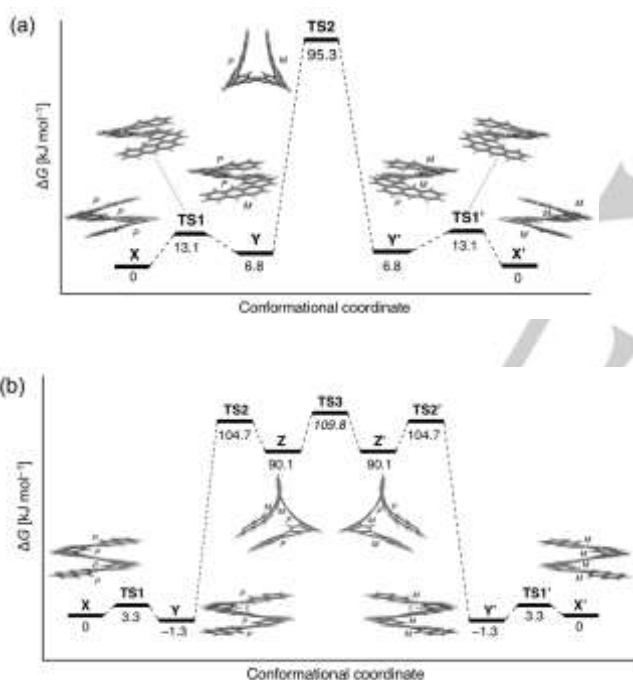


Figure 5. Mechanism of enantiomerization of **[4]HA** (a) and **[5]HA** (b) calculated at M06-2X/6-31(d,p) level. Only energy-minimum structures are shown in the energy profile of **[5]HA**. Transition state structures are shown only for **[4]HA**. P: plus, M: minus, c: nearly coplanar.

In summary, we synthesized compounds **[4]HA** and **[5]HA** by cycloisomerization as anthracene-based expanded helicenes. In contrast to **[3]HA**, there was significant face-to-face stacking between the anthracene units in the structures of **[4]HA** and **[5]HA** at the interlayer distance of ca. 0.33 nm. The presence of significant $\pi\cdots\pi$ interactions was supported by the thermochemical analysis with the homodesmotic reaction as well as characteristic fluorescence properties. DFT calculations showed that the helical inversion of **[4]HA** and **[5]HA** occurred via multistep mechanisms at relatively high barriers. In order to

Acknowledgements

This work was partly supported by JSPS KAKENHI Grant Number JP20H02721 and Nagase Science and Technology Foundation. The authors thank Professor Osamu Ishitani and Dr. Yusuke Tamaki of Tokyo Institute of Technology for the measurements of fluorescence spectra.

Keywords: Arenes • Molecular structure • Electronic spectra • Helical inversion • $\pi\cdots\pi$ interactions

- [1] a) C.-F. Chen, Y. Shen, *Helicene Chemistry: From Synthesis to Applications* Springer, Berlin, **2017**; b) M. Gingras, *Chem. Soc. Rev.* **2013**, *42*, 968–1006; c) Y. Shen, C.-F. Chen, *Chem. Rev.* **2012**, *112*, 1463–1535.
- [2] P. Sehnal, I. G. Stará, D. Šaman, M. Tichý, J. Mišek, J. Cvačka, L. Rulíšek, J. Chocholoušová, J. Vacek, G. Goryl, M. Szymonski, I. Císařová, I. Starý, *Proc. Nat. Acad. Sci. USA* **2009**, *106*, 13169–13174.
- [3] K. Mori, T. Murase, M. Fujita, *Angew. Chem. Int. Ed.* **2015**, *54*, 6847–6851; *Angew. Chem.* **2015**, *127*, 6951–6955.
- [4] K. Fujise, E. Tsurumaki, G. Fukuhara, N. Hara, Y. Imai, S. Toyota, *Chem. Asian J.* **2020**, *15*, 2456–2461.
- [5] G. R. Kiel, S. C. Patel, P. W. Smith, D. S. Levine, T. D. Tilley, *J. Am. Chem. Soc.* **2017**, *139*, 18456–18459.
- [6] Y. Nakakuki, T. Hirose, K. Matsuda, *J. Am. Chem. Soc.* **2018**, *140*, 15461–15469.
- [7] a) I. Warnke, F. Furche, *WIREs Comput. Mol. Sci.* **2012**, *2*, 150–166; b) Y. Nakai, T. Mori, Y. Inoue, *J. Phys. Chem. A* **2013**, *117*, 83–93.
- [8] a) H. Tanaka, Y. Inoue, T. Mori, *ChemPhotoChem* **2018**, *2*, 386–402; b) H. Tanaka, M. Ikenosako, Y. Kato, M. Fujiki, Y. Inoue, T. Mori, *Commun. Chem.* **2018**, *1*, 38; c) N. Chen, B. Yan, *Molecules* **2018**, *23*, 3376.
- [9] a) Y. Nakakuki, T. Hirose, H. Sotome, H. Miyasaka, K. Matsuda, *J. Am. Chem. Soc.* **2018**, *140*, 4317–4326; b) Y. Zhu, Z. Xia, Z. Cai, Z. Yuan, N. Jiang, T. Li, Y. Wang, X. Guo, Z. Li, S. Ma, D. Zhong, Y. Li, J. Wang, *J. Am. Chem. Soc.* **2018**, *140*, 4222–4226; c) C. M. Cruz, S. Castro-

COMMUNICATION

- Fernández, E. Maçôas, J. M. Cuerva, A. G. Campaña, *Angew. Chem. Int. Ed.* **2018**, *57*, 14782–14786; *Angew. Chem.* **2018**, *130*, 14998–15002.
- [10] a) L. Rulišek, O. Exner, L. Cwiklik, P. Jungwirth, I. Starý, L. Pospíšil, Z. Havlas, *J. Phys. Chem. C* **2007**, *111*, 14948–14955; b) C.-B. Huang, A. Ciesielski, P. Samorì, *Angew. Chem. Int. Ed.* **2020**, *59*, 7319–7330; *Angew. Chem.* **2020**, *132*, 7387–7398.
- [11] a) W. H. Laarhoven, Th. J. H. M. Cuppen, R. J. F. Nivard, *Tetrahedron* **1970**, *26*, 4865–4881; b) R. G. Harvey, *Polycyclic Aromatic Hydrocarbons*, Wiley-VCH, New York, **1997**, chap. 6.1.17.
- [12] T. A. Manes, M. J. Rose, *Inorg. Chem.* **2016**, *55*, 5127–5138.
- [13] a) A. Fürstner, V. Mamane, *J. Org. Chem.* **2002**, *67*, 6264–6267; b) V. Mamane, P. Hannen, A. Fürstner, *Chem. Eur. J.* **2004**, *10*, 4556–4575; c) J. Carreras, M. Patil, W. Thiel, M. Alcarazo, *J. Am. Chem. Soc.* **2012**, *134*, 16753–16758.
- [14] All ¹H NMR signals were assigned by the 2D NMR spectra.
- [15] Y. Nakai, T. Mori, Y. Inoue, *J. Phys. Chem. A* **2012**, *116*, 7372–7385.
- [16] a) Y. Zhao, D. G. Truhlar, *Chem. Phys. Lett.* **2011**, *502*, 1–13; b) Y. Zhao, D. G. Truhlar, *Acc. Chem. Res.* **2008**, *41*, 157–167. The structure of [4]HA was optimized by using various functionals and basis sets (Table S3).
- [17] a) S. Toyota, K. Wakamatsu, *Bull. Chem. Soc. Jpn.* **2020**, *93*, 65–75; b) S. Toyota, K. Wakamatsu, T. Kawakami, T. Iwanaga, *Bull. Chem. Soc. Jpn.* **2015**, *88*, 283–291.
- [18] HOMA and NICS (nucleus-independent chemical shift) values of the C₂ symmetric structures of [4]HA and [5]HA are given in Supporting Information. We also calculated the structure of [6]HA (Figure S8), where the number of turns was ca. 1.8 in the C₂ symmetric structure.
- [19] S. E. Wheeler, K. N. Houk, P. v. R. Schleyer, W. D. Allen, *J. Am. Chem. Soc.* **2009**, *131*, 2547–2560.
- [20] a) R. Podeszwa, K. Szalewicz, *Phys. Chem. Chem. Phys.* **2008**, *10*, 2735–2746; b) C. Gonzalez, E. C. Lim, *J. Phys. Chem. A* **2003**, *107*, 10105–10110.
- [21] NCIPLOT4. a) R. A. Boto, F. Peccati, R. Laplaza, C. Quan, A. Carbone, J.-P. Piquemal, Y. Maday, J. Contreras-García, *J. Chem. Theory Comput.* **2020**, *16*, 4150–4158; b) J. Contreras-García, E. R. Johnson, S. Keinan, R. Chaudret, J.-P. Piquemal, D. N. Beratan, W. Yang, *J. Chem. Theory Comput.* **2011**, *7*, 625–632; c) E. R. Johnson, S. Keinan, P. Morisánchez, J. Contreras-García, A. J. Cohen, W. Yang, *J. Am. Chem. Soc.* **2010**, *132*, 6498–6506.
- [22] An irregularly large fluorescence quantum yield and a long-lived fluorescence of [2]HA cannot be explained from available data and will be investigated elsewhere.
- [23] a) B. Valeur, M. N. Berberan-Santos "Molecular Fluorescence: Principles and Applications, 2nd ed." Wiley-VCH, Weinheim, **2012**, chap. 6.4; b) S. Toyota, M. Goichi, M. Kotani, *Angew. Chem., Int. Ed.* **2004**, *43*, 2248–2251; *Angew. Chem.* **2004**, *116*, 2298–2301.
- [24] a) M. Buchta, J. Rybáček, A. Jančařík, A. A. Kudale, M. Buděšínský, J. V. Chocholoušová, J. Vacek, L. Bednářová, I. Čísařová, G. J. Bodwell, I. Starý, I. G. Stará, *Chem. Eur. J.* **2015**, *21*, 8910–8917; b) Y. Hu, G. M. Paternò, X.-Y. Wang, X.-C. Wang, M. Guizzardi, Q. Chen, D. Schollmeyer, X.-Y. Cao, G. Cerullo, F. Scotognella, K. Müllen, A. Narita, *J. Am. Chem. Soc.* **2019**, *141*, 12797–12803.
- [25] a) J. Barroso, J. L. Cabellos, S. Pan, F. Murillo, X. Zarate, M. A. Fernandez-Herrera, G. Merino, *Chem. Commun.* **2018**, *54*, 188–191; b) R. H. Janke, G. Haufe, E.-U. Würthwein, J. H. Borkent, *J. Am. Chem. Soc.* **1996**, *118*, 6031–6035; c) S. Grimme, S. D. Peyerimhoff, *Chem. Phys.* **1996**, *204*, 411–417.

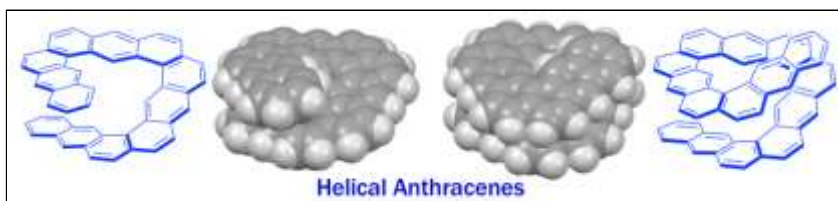
COMMUNICATION

Entry for the Table of Contents

Helical Molecules

K. Fujise, E. Tsurumaki, K. Wakamatsu, S. Toyota*

Construction of helical structures with multiple fused anthracenes: structures and properties of long expanded helicenes



Helical structures are lengthened by fusing of four and five anthracene units. Significant interlayer $\pi \cdots \pi$ interactions are evidenced by molecular structures and spectroscopic data.

Institute and/or researcher Twitter usernames: ((optional))